The role of topography on catchment-scale water residence time

K. J. McGuire,[1,2] J. J. McDonnell,[1] M. Weiler,[3] C. Kendall,[4] B. L. McGlynn,[5]
J. M. Welker,[6] and J. Seibert[7]

Received 16 September 2004; revised 1 February 2005; accepted 14 February 2005; published 3 May 2005.

[1] The age, or residence time, of water is a fundamental descriptor of catchment hydrology, revealing information about the storage, flow pathways, and source of water in a single integrated measure. While there has been tremendous recent interest in residence time estimation to characterize watersheds, there are relatively few studies that have quantified residence time at the watershed scale, and fewer still that have extended those results beyond single catchments to larger landscape scales. We examined topographic controls on residence time for seven catchments (0.085–62.4 km^2) that represent diverse geologic and geomorphic conditions in the western Cascade Mountains of Oregon. Our primary objective was to determine the dominant physical controls on catchment-scale water residence time and specifically test the hypothesis that residence time is related to the size of the basin. Residence times were estimated by simple convolution models that described the transfer of precipitation isotopic composition to the stream network. We found that base flow mean residence times for exponential distributions ranged from 0.8 to 3.3 years. Mean residence time showed no correlation to basin area ($r^2 < 0.01$) but instead was correlated ($r^2 = 0.91$) to catchment terrain indices representing the flow path distance and flow path gradient to the stream network. These results illustrate that landscape organization (i.e., topography) rather than basin area controls catchment-scale transport. Results from this study may provide a framework for describing scale-invariant transport across climatic and geologic conditions, whereby the internal form and structure of the basin defines the first-order control on base flow residence time.

Citation: McGuire, K. J., J. J. McDonnell, M. Weiler, C. Kendall, B. L. McGlynn, J. M. Welker, and J. Seibert (2005), The role of topography on catchment-scale water residence time, *Water Resour. Res.*, *41*, W05002, doi:10.1029/2004WR003657.

1. Introduction

[2] The process conception of water flow paths and storages in catchment hydrology has been largely influenced by detailed field investigations at disparate site locations. This has limited our capability to develop scaling relationships that are consistent with the complex hydrological processes observed at these sites and elsewhere in nature. The organization of field observations into a hierarchy of importance at different scales has proven difficult [*Bonell*, 1998; *Sidle et al.*, 2000; *Sivapalan*, 2003] and characterizing even simple, extremely well instrumented hillslopes and small catchments has been a challenge for hydrologists [*Anderson et al.*, 1997; *Hooper*, 2001; *McGlynn et al.*, 2002]. This fact has hindered the ability to explain and predict how patterns and processes change across scale. Ultimately, advances in measurement technologies and field observations lag behind the current theoretical framework to scale hydrological processes, which questions how process-level observation can be used in mesoscale (e.g., 100 to 1000 km^2) modeling efforts and management programs. Many properties for which scaling relationships have been developed do not lend themselves to verification, since properties such as hydraulic conductivity measured at small scales (e.g., 0.1 to 10s m^2) become effective properties determined through model calibration at larger scales.

[3] Tracers have provided some of the most important insights into hydrological processes; from the definition of groundwater and surface water age, to hydrograph source components, to descriptions of water flow pathways at the larger integrative catchment scale [*Dinçer and Davis*, 1984; *Buttle*, 1994; *Kendall and McDonnell*, 1998; *McDonnell et al.*, 1999; *Uhlenbrook et al.*, 2002; *Soulsby et al.*, 2004]. Therefore tracer techniques provide an opportunity to examine how flow systems scale based on field observations that describe mechanisms operating within catchments. Tracers allow us to estimate the age or residence time of water in the catchment, revealing information about the storage, flow pathways and source of water in a single measure. Stable isotopes of water (^{18}O and ^{2}H) have been used for the estimation of residence times of <5 years, while

[1]Department of Forest Engineering, Oregon State University, Corvallis, Oregon, USA.
[2]Now at School of Civil and Environmental Engineering, Georgia Institute of Technology, Atlanta, Georgia, USA.
[3]Department of Forest Resources Management, University of British Columbia, Vancouver, British Columbia, Canada.
[4]U.S. Geological Survey, Menlo Park, California, USA.
[5]Department of Land Resources and Environmental Sciences, Montana State University, Bozeman, Montana, USA.
[6]Environment and Natural Resources Institute and Department of Biology, University of Alaska Anchorage, Anchorage, Alaska, USA.
[7]Department of Physical Geography and Quaternary Geology, Stockholm University, Stockholm, Sweden.

Copyright 2005 by the American Geophysical Union.
0043-1397/05/2004WR003657

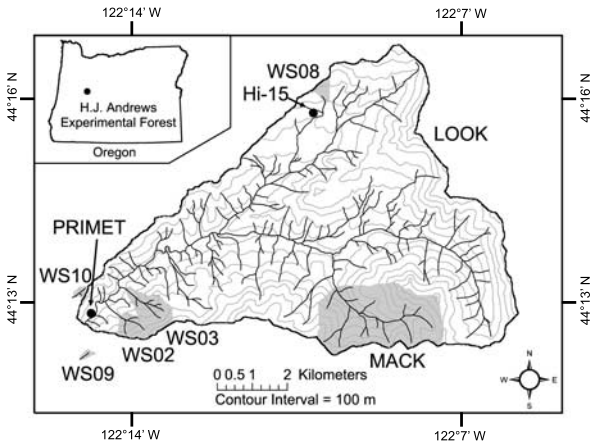

Figure 1. Map of the H.J. Andrews Experimental Forest showing the locations of the study catchments.

tritium (^{3}H) is often used to estimate residence times >5 years [*DeWalle et al.*, 1997; *Maloszewski et al.*, 1983; *Uhlenbrook et al.*, 2002].

[4] The residence time (or distribution of residence times) of water draining a catchment not only has important implications for flow pathways and storage, but for its water quality, since many biogeochemical reactions are time-dependent [e.g., *Hornberger et al.*, 2001; *Burns et al.*, 2003]. The contact time with subsurface materials has direct control on chemical composition and biogeochemical processes. Additionally, the residence time indicates the catchment's memory to past inputs and can thus be used as a proxy to understand the hydrologic sensitivity to land use and climate change and other impacts such as its vulnerability to contamination. Understanding how residence time scales is crucial for a variety of biogeochemical and hydrological applications.

[5] Knowledge of how residence time scales would also help illuminate processes that control subsurface flow routing since the residence time is directly related to the diversity of flow pathways in a catchment [*Pearce et al.*, 1986; *McDonnell et al.*, 1991; *Kirchner et al.*, 2001]. Describing processes for large-scale catchments is necessary for developing more understanding-based models that can be used to address questions of practical importance at scales that affect land management and climate change issues. The challenge is how we define model structures for mesoscale prediction where observations may be limited [*Sivapalan*, 2003]. Residence times can be used to constrain parameterizations for storage in conceptual rainfall-runoff models and provide a process basis for the structure of the model [*Uhlenbrook et al.*, 2000]. The incorporation of residence time estimates and their uncertainty may lead to better predictions of water and solute flux from hydrological models.

[6] While there has been tremendous recent interest in residence time estimation to characterize catchments [e.g., *Gibson et al.*, 2002; *Hooper*, 2004], there are relatively few studies that have quantified residence time at the catchment scale, and fewer still that have extended those results beyond single catchments to larger landscape scales. We argue that the relationships between stream water residence time and landscape characteristics provide an opportunity to transfer information from one spatial scale to another. However, the scaling of residence time has been only recently addressed in a few studies [*McGlynn et al.*, 2003; *Rodgers et al.*, 2005]. *McGlynn et al.* [2003] did not find a relationship with catchment scale and residence time, but with the nature of area accumulation within catchments. Only four catchments were evaluated in their study; however, results from *Rodgers et al.* [2005] provide further support that residence time does not scale with catchment size. Several studies have also examined the residence time of water in hillslopes and found a dependence on accumulated area [*Stewart and McDonnell*, 1991; *Rodhe et al.*, 1996] and contribution of bedrock seepage [*Asano et al.*, 2002]. These studies suggest that the controls on catchment-scale residence time are complex.

[7] In this paper, residence time is estimated for a set of seven nested catchments using simple flow models that interpret stable isotope variations of rainfall and runoff. We use the results from residence time models to address the following questions: (1) Is stream water residence time related to the size of the catchment? (2) Does topography exert a control on the residence time? (3) Is there a relationship that links residence time across scale? Our primary objective was to determine the dominant control on catchment-scale residence time and provide a simple framework to regionalize those results within a mesoscale basin (62 km^2).

2. Site Description

[8] The study catchments are located within the H.J. Andrews Experimental Forest (HJA) in the central western Cascades of Oregon, USA (44.2°N, 122.2°W) (Figure 1). The main drainage within the HJA is Lookout Creek (LOOK, 62.42 km^2), which is a tributary to Blue River and eventually the McKenzie River within the Willamette River Basin. Past hydrologic investigations at HJA have focused on the effects of forest management activities on water yield [*Rothacher*, 1965], peak flows [*Harr and McCorison*, 1979; *Jones and Grant*, 1996], snowmelt and accumulation [*Harr*, 1986; *Berris and Harr*, 1987], and catchment nutrient budgets [*Sollins et al.*, 1980]. Detailed site descriptions of the overall HJA and the small basins are given by *Rothacher et al.* [1967], *Jones and Grant* [1996], and *Jones* [2000].

[9] Catchments areas (see Figure 1) range from 0.085 to 62.42 km^2 and span the climatic, geomorphic, and topographic settings found within the overall LOOK basin (see Table 1). This study focuses on seven catchments within the HJA (WS02, WS03, WS08, WS09, WS10, MACK, and LOOK). While WS09 and WS10 lie immediately outside of LOOK, they represent catchments of similar drainage area and geomorphology to those contained in the lower portion of LOOK.

[10] Lower elevation areas are dominated by Douglas fir (*Pseudotsuga menziesii*), western hemlock (*Tsuga heterophylla*), and western redcedar (*Thuja plicata*) and upper elevation forests contain noble fir (*Abies procera*), Pacific silver fir (*Abies amabilis*), Douglas fir, and western hemlock. The coniferous forest landscape is underlain at its lower elevation (<760 m) by mainly Oligocene-lower Miocene formations of volcanic origin, consisting of massive

Table 1. Geologic and Geomorphic Catchment Descriptions

Catchment	Area, km^2	Mean Slope, deg	Minimum Elevation, m	Maximum Elevation, m	Geologic/Geomorphic Description[a]
WS02	0.601	27	548	1070	97% steep volcaniclastics, 3% fractured andesitic/basaltic lava flows and soils <1 m
WS03	1.011	26	418	1080	68% steep volcaniclastics with <1 m soils, 22% earthflow with >3 m soils, 10% fractured andesitic/basaltic lava flows
WS08	0.214	15	993	1170	55% Benchy volcaniclastics and glaciated till/colluvium, 45% earthflow with >3 m soils, 24% glaciated till/colluvium
WS09	0.085	31	432	700	99% steep volcaniclastics with <1 m soils
WS10	0.102	29	473	680	92% steep volcaniclastics, with basaltic/rhyolitic dikes and 1–3 m soils
MACK	5.81	25	758	1610	82% steep volcaniclastics with <1 m soils, 18% fractured andesitic/basaltic lava flows
LOOK	62.42	20	428	1620	all of the above including large alluvial stream terraces, ~1–3 m soils

[a]Information compiled from a variety of resources including *Swanson and James* [1975], *Legard and Meyer* [1973], *Dyrness* [1969], and *Harr* [1977].

tuffs and breccias derived from mudflows and pyroclastic flows [*Swanson and James*, 1975]. In higher-elevation areas (>1200 m), bedrock is composed of andesitic and basaltic lava flows of Pliocene age [*Sherrod and Smith*, 2000]. The intermediate elevations transition from welded and non-welded ash flows to basalt and andesite lava flows. Additionally, glacial, alluvial, and mass movement processes have created deeply dissected, locally steep drainage systems and variable regolith depth [*Swanson and James*, 1975]. Hillslopes of the lower-elevation catchments (e.g., WS02, WS03, WS09, and WS10) are short (<200 m) and steep (22 to 48°), with local relief of between 60–130 m. Upper elevation catchments (e.g., WS08) are characterized by more gentle (11 to 22°), longer hillslopes (>250 m).

[11] Soils are mainly poorly developed Inceptisols with local areas of Alfisols and Spodosols containing thick organic horizons that have developed over highly weathered parent materials [*Dyrness*, 1969; *Legard and Meyer*, 1973; *Ranken*, 1974]. Although the <2 mm soil fractions are generally composed of a clay loam texture, the soils exhibit massive well aggregated structure that affect hydrologic properties: high infiltration rates (typically >500 cm/h), high drainable porosity (between 15% and 30%), and sharply declining water retention curves [*Dyrness*, 1969; *Ranken*, 1974; *Harr*, 1977]. Overland flow has not been observed on soils in any of the watersheds.

[12] Average annual precipitation varies with elevation from about 2300 mm at the base to over 3550 mm at upper elevations, falling mainly between November and April (~80% of annual precipitation) during frequent long-duration, low- to moderate-intensity frontal storms. The Mediterranean climate has wet, mild winters and exceptionally dry, cool summers. Low-elevation (430 m) mean monthly temperature ranges from near 1°C in January to 18°C in July. Rainfall predominates at low elevations and snow is more common at higher elevations (e.g., WS08 and MACK). On average, 56% (28 to 76%) of the annual precipitation becomes runoff, which is highly responsive and dominated by average quickflow ratios (38%) that are among the highest reported in the literature [e.g., *Hewlett and Hibbert*, 1967; *McGlynn et al.*, 2002].

3. Methodology

3.1. Field Measurements

[13] Precipitation samples were collected weekly from January 2000 to February 2003 (~1130 day period) in bulk collectors at two locations that coincided with a low (PRIMET, 430 m) and high (Hi-15, 922 m) elevation meteorological station. Precipitation samplers consisted of plastic funnels with drainage tubing attached to plastic bottles. To minimize evaporation, water traps were created by looping drainage tubes and protecting collection bottles in either a climate controlled shelter (Hi-15) or by burying the bottle beneath the soil surface below a small insulated shelter (PRIMET). Precipitation rates were determined using heated tipping bucket rain gauges at each station as part of HJA long-term data collection. Snowmelt sampling occurred weekly at Hi-15 during the 2001–2002 winter using a 0.25 m^2 snow lysimeter that drained into a heated shelter to prevent the samples from freezing. Snowmelt rates were measured using tipping buckets (0.025 mm per tip) and a 5.52 m^2 lysimeter. A network of small bulk rainfall collectors (N = 38) were used to assess input variations across the large basin scale for 3 rain storms in fall 2002. Seven stream sites (WS02, WS03, WS08, WS09, WS10, MACK, and LOOK) were sampled weekly (generally on the same day as precipitation sample collection). Since weekly precipitation samples represent volume-weighted averages over the preceding week, samples that were collected within a 24-hr window of an event were not used in the analysis. Therefore the following analysis pertains only to timescales longer than one week.

[14] Samples collected prior to October 2000 were analyzed at the Colorado State University facility for Mass Spectrometry and after October 2000, at the USGS Stable Isotope Laboratory in Menlo Park, California for oxygen-18 composition ($\delta^{18}O$) using an automated version of the CO_2–H_2O equilibration technique of *Epstein and Mayeda* [1953]. The $\delta^{18}O$ values are reported in per mil (‰) relative to a standard as $\delta^{18}O = (R_x/R_s - 1) \times 1000$, where R_x and R_s are the $^{18}O/^{16}O$ ratios for the sample and standard (VSMOW), respectively. The analytical precision (σ) was 0.11‰ based on submitted blind duplicate samples.

3.2. Input Characterization

[15] The input $\delta^{18}O$ for each catchment was adjusted for an elevation effect [cf. *Dansgaard*, 1964] based on the two (high/low elevation) sampling stations. For catchments with significant seasonal snowpack (WS08, MACK, and LOOK), the Hi-15 station was used as the reference input signal, which included snowmelt rates and isotopic composition when a snowpack was present, while low-elevation catchments (WS02, WS03, WS09, and WS10) used the PRIMET station as the reference input signal. The input

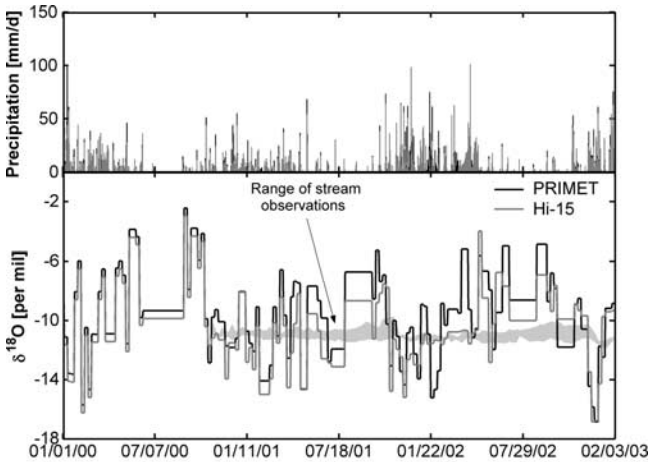

Figure 2. Daily precipitation and weekly δ^{18}O measured at PRIMET (430 m) and Hi-15 (922 m) meteorological stations. The shaded area shows that range of measured streamflow δ^{18}O for all catchments.

δ^{18}O used for each basin was adjusted depending on the isotopic difference between the two precipitation stations for each of the sampling periods. This was computed as a simple linear interpolation:

$$\delta_{in}(t) = (E_R - E_{ref})S(t) + \delta^{18}\mathrm{O}_{ref}(t) \tag{1}$$

where δ_{in} is the catchment specific δ^{18}O input, E_R is the effective catchment recharge elevation and a fitting parameter, E_{ref} is the elevation of the reference precipitation station, S is the isotopic difference between Hi-15 and PRIMET stations normalized by their elevation difference, and $\delta^{18}\mathrm{O}_{ref}$ is the measured isotopic composition for the reference station. The isotopic difference term S is time-dependent (i.e., varies with sample collection period), since the elevation effect can vary in time. When a catchment effective recharge elevation equals the elevation of the reference precipitation station, then the measured isotopic composition for that station is used as input for that catchment. An elevation effect is only invoked when a calibrated effective recharge elevation is greater than the elevation of the reference precipitation station.

[16] Residence time studies often suffer from short input records, which yield nonunique model calibrations or uncertain parameter estimates of the residence time distribution. Many investigators have extended stable isotope inputs using regression models with temperature records [*Burns and McDonnell*, 1998; *Uhlenbrook et al.*, 2002], annual sinusoidal components [*McGuire et al.*, 2002], or data from nearby long-term stations [*Maloszewski et al.*, 1992; *Vitvar and Balderer*, 1997]. In our study, complex topography and the lack of strong seasonal δ^{18}O fluctuations in precipitation precluded the two latter approaches. We examined several regression models based on temperature, precipitation, wind direction (a surrogate for storm track), and interactions of these variables, but at best could not explain more than 30% of the observed δ^{18}O variation. Inputs prior to January 2000 were roughly approximated by assuming that the mean base flow (i.e., groundwater) δ^{18}O of each catchment reflects the long-term average input δ^{18}O. In general, the seasonality of precipitation limits recharge to the winter; thus causing an effectively constant δ^{18}O input. A warm-up period of ten months was used to minimize potential effects of the assumed constant input on the residence time calibration (see the range of measured streamflow δ^{18}O in Figure 2). The past inputs allowed us to examine residence times that were greater than the length of time for which precipitation δ^{18}O was measured (~1130 days). It can be shown for all sites where there is no elevation effect on the precipitation δ^{18}O, that the long-term weighted δ^{18}O of precipitation is approximately equal to the mean base flow composition. Precipitation sampled at PRIMET in this study and by *Welker* [2000] had a weighted mean δ^{18}O of −10.46‰. The base flow mean δ^{18}O for corresponding sites (i.e., similar elevation) was −10.61 and −10.84‰ for WS09 and WS10, respectively. At the high-elevation site (Hi-15), the weighted mean δ^{18}O was −11.43‰ which was comparable to the mean base flow δ^{18}O in WS08 of −11.27‰.

3.3. Residence Time Modeling Theory and Approach

[17] The tracer composition of precipitation that falls on a catchment will be delayed by some timescale(s) before reaching the stream. More explicitly, the stream outflow composition at any time, $\delta_{out}(t)$, consists of past inputs lagged, $\delta_{in}(t - \tau)$, according to their residence time distribution, $g(\tau)$ [*Dinçer et al.*, 1970; *Maloszewski and Zuber*, 1982; *Richter et al.*, 1993]:

$$\delta_{out}(t) = \int_0^\infty g(\tau)\delta_{in}(t-\tau)d\tau \tag{2}$$

where τ are the lag times between input and output tracer composition. This model is similar to the linear system approach used in unit hydrograph models [e.g., *Dooge*, 1973]; however, only tracer is considered here and thus $g(\tau)$ represents the tracer transfer function (see discussion below). Equation (2) is valid only for systems at steady state or when the mean flow pattern does not change significantly in time [*Zuber*, 1986]. It can be reexpressed with both t and τ corrected as flow time [*Rodhe et al.*, 1996]:

$$t_c = \int_0^t Q(t)dt/\overline{Q} \tag{3}$$

where t_c is flow-corrected time and $\overline{Q}$ is the mean annual flow. Accordingly, the assumption of time invariance holds, since t_c is proportional to the flow rate relative to the mean annual flow. We used both expressions of time in equation (2) and obtained similar fits to our stream isotope data. *Kirchner et al.* [2000, 2001] also found that a similar time transformation yielded equivalent results to equation (2). Therefore, in this study we used the strict time-based approach since interpretation is more straightforward. This assumes an average residence time distribution for the study period, even though the precipitation seasonality suggests a time variant distribution. However, because the temporal precipitation

Table 2. Descriptions of Residence Time Distributions

Model	Residence Time Distribution $g(\tau)$	Parameters	Mean Residence Time[a]
Exponential[b]	$\tau_m^{-1}\exp(-\tau/\tau_m)$	τ_m	τ_m
Exponential-piston flow[b]	$\left(\frac{\tau_m}{\eta}\right)^{-1}\exp\left(-\frac{\eta\tau}{\tau_m}+\eta-1\right)$ for $\tau \geq \tau_m(1-\eta^{-1})$	τ_m, η	τ_m
	0 for $\tau < \tau_m(1-\eta^{-1})$		
Dispersion[b]	$\left(\frac{4\pi D_p\tau}{\tau_m}\right)^{-1/2}\tau^{-1}\times\exp\left[-\left(1-\frac{\tau}{\tau_m}\right)^2\left(\frac{\tau_m}{4D_p\tau}\right)\right]$	τ_m, D_p[c]	τ_m
Gamma[d]	$\frac{\tau^{\alpha-1}}{\beta^\alpha\Gamma(\alpha)}\exp(-\tau/\beta)$	α, β	$\alpha\beta$
Two parallel linear reservoirs[e]	$\frac{\phi}{\tau_f}\exp\left(-\frac{\tau}{\tau_f}\right)+\frac{1-\phi}{\tau_s}\exp\left(-\frac{\tau}{\tau_s}\right)$	τ_f, τ_s, ϕ	–
Power law[f]	$\frac{\tau^k}{\Gamma(1-k)}$	k	–

[a]No characteristic residence time is associated with the power law model; the two parallel linear reservoirs model was calculated numerically by the first moment.
[b]*Maloszewski and Zuber* [1982].
[c]D_p = 1/Peclet number.
[d]*Kirchner et al.* [2001].
[e]*Weiler et al.* [2003].
[f]*Schumer et al.* [2003].

pattern is the same for all catchments, the results are relatively comparable.

[18] The convolution equation (2) must also include recharge weighting $w(t-\tau)$ so that the streamflow composition reflects the mass flux leaving the catchment [*Stewart and McDonnell*, 1991; *Weiler et al.*, 2003]:

$$\delta_{out}(t) = \frac{\int_0^\infty g(\tau)w(t-\tau)\delta_{in}(t-\tau)d\tau}{\int_0^\infty g(\tau)w(t-\tau)d\tau} \quad (4)$$

This modification is more flexible than other recharge adjustment techniques [*Grabczak et al.*, 1984; *Maloszewski et al.*, 1992] and allows for any appropriate factor to be used such as rainfall rates, throughfall rates, or partially weighted rainfall rates (e.g., effective rainfall). In our case, measured daily precipitation/snowmelt rates were used for $w(t)$ since the seasonality of precipitation/snowmelt and recharge are strongly correlated at HJA. Nonetheless, we examined more complex models to estimate effective precipitation using simple rainfall-runoff transfer functions (i.e., unit hydrograph approaches [see *Weiler et al.*, 2003]), but these did not yield different residence times and the increased number of parameters increased the overall model uncertainty. Different realizations of the recharge term had little effect on the estimates of residence time. This is likely an effect of the Mediterranean climate, where the high evapotranspiration demand coincides with a period of little rainfall. From equation (4) (and (2)) it is clear that $g(\tau)$ must sum to unity to conserve mass.

[19] The travel time or residence time distribution (RTD or $g(\tau)$) describes the fractional weighting of how mass (i.e., tracer) exits the system, which is equivalent to the probability density function (pdf) or transfer function of tracer applied to the catchment. If the tracer is conservative and there are no immobile zones in the catchment, then the tracer RTD is equal to the water RTD or the mean residence time of tracer is equal to the mean residence time of water (V_m/Q, where V_m is the volume of mobile water and Q is the volumetric flow rate through the system). Our definition of residence time herein is the time elapsed since the water molecule entered the catchment as recharge to when it exits at some discharge point (i.e., catchment outlet, monitoring well, soil water sampler, etc.) [*Bethke and Johnson*, 2002; *Etcheverry and Perrochet*, 1999; *Rodhe et al.*, 1996]. RTDs used in equations (2) and (4) are time-invariant, spatially lumped characteristics of the catchment.

[20] It is important to note that the timescale of the runoff response is different than the residence time because fluctuations in hydraulic head (the driving force in water flux) can propagate much faster than the transport of conservative tracer or individual water molecules [see *Weiler et al.*, 2003]. Thus the timescales between the rainfall-runoff response and transport (i.e., residence time) are effectively decoupled [*Williams et al.*, 2002]. This partially explains why the majority of a storm flow hydrograph is composed of 'old' water [*Buttle*, 1994; *Richey et al.*, 1998; *Kendall and McDonnell*, 1998] even though runoff response to rainfall is often immediate [*Kirchner*, 2003].

[21] A catchment's RTD could have various shapes depending on the exact nature of its flow path distribution and flow system. Distributions that were evaluated in this study are shown in Table 2. They include the exponential and exponential-piston flow distributions, which represent the apparent behavior of a well-mixed linear reservoir or a delayed linear reservoir, respectively [*Maloszewski and Zuber*, 1982; *Rodhe et al.*, 1996]. The exponential distribution is the most widely used distribution in catchment systems [*Haitjema*, 1995; *DeWalle et al.*, 1997; *Amin and Campana*, 1996; *Burns et al.*, 1998; *Buttle et al.*, 2001]. Other distributions such as the dispersion and gamma have been used successfully in several catchment studies as well [*Maloszewski and Zuber*, 1982; *Maloszewski et al.*, 1983; *Vitvar and Balderer*, 1997; *Kirchner et al.*, 2000]. The dispersion distribution is the one-dimensional solution to

the advection-dispersion equation assuming that tracer is introduced and sampled in proportion to volumetric flow [*Kreft and Zuber*, 1978]. The gamma distribution, which has been used widely in unit hydrograph modeling [cf. *Dooge*, 1973], was demonstrated by *Kirchner et al.* [2000] to consistently represent the RTD for several catchments in Wales. Using a spectral analysis technique (i.e., convolution (equation (2)) in the frequency domain), they found that the shape parameter, α, for the gamma distribution (see Table 2) was approximately 0.5 implying that catchments act as fractal frequency filters at timescales ca. <2 to 3 years. We also tested a simple, less flexible (i.e., one parameter) power law distribution (see Table 2, power law model) and two exponential distributions in parallel (as described by *Weiler et al.* [2003]).

[22] We used a reflective Newton nonlinear least squares algorithm in MATLAB® to solve the inverse estimation problem of parameter identification for the distributions described above [*Coleman and Li*, 1994]. We found the set of parameters that minimized the sum of squared residual errors between the modeled and observed stream $\delta^{18}O$. A first-order linear approximation to the parameter variance-covariance matrix ($\hat{V}$) is [*Donaldson and Schnabel*, 1987; *Ratkowsky*, 1990]:

$$\hat{V} = s^2\left(J^T J\right)^{-1} \tag{5}$$

where s^2 is the estimated residual variance between the model simulation and observations and J is the Jacobian, which is the matrix of sensitivities of the model output to the parameter estimates. Parameter estimate standard deviations (σ_p) were computed from the square root of the respective diagonal from $\hat{V}$ [*Haggerty et al.*, 2001]. Approximate 95% confidence limits on parameter estimates were taken as $2\sigma_p$. For purposes of model comparison, we used the efficiency (E) proposed by *Nash and Sutcliffe* [1970] and the root mean square error (RMSE) corrected for the number of parameters estimated [*Bard*, 1974]. Other measures such as parameter/objective function scattergrams and temporal sensitivity plots [*Knopman and Voss*, 1987] were used to evaluate overall model performance but are not directly reported in this paper.

3.4. Topographic Analysis

[23] A 10 m digital elevation model (DEM) was used to compute topographic attributes for each of the 7 seven HJA catchments. Stream networks were determined using a channel-threshold area method. On the basis of observations in several of the small basins, 0.5 ha was used as an initiation area in order to achieve an adequate number of channels at the small basin scale. This threshold area is comparable to other studies in similar topographic systems [*Montgomery and Dietrich*, 1988; *McGlynn and Seibert*, 2003]. We used the 0.5 ha threshold for all basins to provide consistency when comparing catchments.

[24] An accumulated area grid was computed using a multidirectional flow algorithm to derive the stream channel network [*McGlynn and Seibert*, 2003]. Then, a single direction flow algorithm was used to compute flow path length and flow path gradient distributions representing the distance and gradient along each flow line to where it enters the stream network. Likewise, the local subcatchment area for each stream segment (i.e., flagged stream cells) was computed to determine the subcatchment area distribution for each basin [*McGlynn and Seibert*, 2003; *McGlynn et al.*, 2003]. Since these distributions are typically skewed, we used median values to characterize each basin. Other basic topographic attributes were computed such as the mean slope, hysometric integral (i.e., the integration of the cumulative frequency distribution of catchment elevations) [*Chorley et al.*, 1985; *Strahler*, 1952], and topographic index (i.e., $\ln(a/\tan\beta)$, where a is upslope accumulated area and β is the local slope angle) [*Beven and Kirkby*, 1979]. We then compared these descriptions of internal catchment form at each catchment scale to estimated mean residence times to explore possible relationships (correlation) with catchment topographic organization.

4. Results

4.1. Spatial and Temporal Isotopic Patterns of Precipitation and Streamflow

[25] Precipitation amounts were generally similar between Hi-15 and PRIMET (equal weekly means, p value = 0.08) with slightly more precipitation at the higher-elevation site (Hi-15). The weekly precipitation totals based on the isotope sample collection dates ranged from 0 to 224 mm. Winter (November to April) average weekly amounts were 68 mm and summer (May to Oct.) average weekly amounts were 24 mm. Both sites had significant seasonal patterns of $\delta^{18}O$ with approximate annual periodic fluctuations ranging over of 8‰ for the years 2000 and 2002 (Figure 2). The 2001 period was drier and warmer than average reflecting the more damped isotopic pattern. The Hi-15 isotopic composition, which included snowmelt, was more depleted in ^{18}O than PRIMET, on average by −0.83‰ (±0.39‰).

[26] Spatial variations in rainfall amount and isotopic composition also indicated strong elevation effects (Figure 3). The largest storm sampled spatially (16–17 September) had rainfall amounts that ranged from 19.2 to 75.8 mm (mean = 34 mm). The second and third storms that were sampled were smaller events (mean = 22.9 and 12.2 mm for 29 September to 1 October and 3–5 October, respectively) and had less overall variation (range = 14.7 to 49.1 mm and 5.1 to 18.2 mm for 29 September to 1 October and 3–5 October, respectively). The variation of the storm isotopic composition was −9.7 to −5.6‰, −14.1 to −6.7‰, and −9.5 to −6.9‰, respectively for each storm. Elevation effects for rainfall determined by regression analysis between $\delta^{18}O$ and station elevation were −0.24‰ per 100 m (rise in elevation) ($r^2 = 0.64$), −0.26‰ per 100 m ($r^2 = 0.89$), and −0.22‰ per 100 m ($r^2 = 0.84$), respectively for each of the three storms. While only synoptic evidence of strong elevation effects, these data indicated that the input composition for each catchment was temporally unique and therefore required elevation adjustment (equation (1)).

[27] The mean elevation effect between weekly input measurements (rain + snowmelt) at PRIMET and Hi-15 was −0.15‰ per 100 m. This is consistent with values reported in the literature [*Clark and Fritz*, 1997]. The weekly elevation effect ($S \times 100$) varied from −1.09‰ per 100 m to 0.78‰ per 100 m, although 90% of the time the values were between −0.22‰ and 0.080‰. Positive

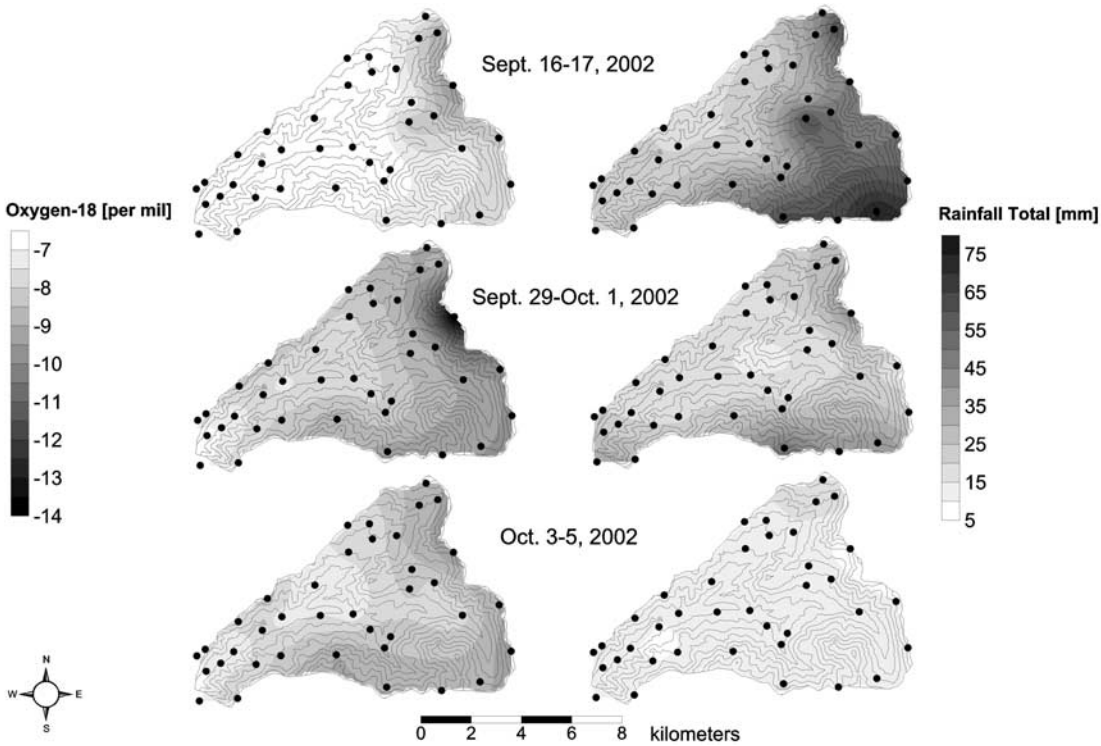

Figure 3. Spatial patterns of (right) total storm rainfall and (left) $\delta^{18}O$ for three synoptically sampled events during the fall 2002. The circles indicate the location of bulk samplers used to collect rainfall.

values were typical when the upper elevations were snow covered and melt isotopic composition was muted compared to lower-elevation, cold temperature rainfall (see winter 2001–2002 in Figure 2). Also, cold air drainage, which has a tendency to affect the PRIMET station (C. Daly, personal communication, 2003), could potentially play a role in isotopic fractionation differences between the two monitoring stations, as well as moisture source, rainout history, and rainfall intensity isotopic effects [*Ingraham*, 1998].

[28] Snowmelt sampled at Hi-15 between 11 December 2001 and 30 April 2002 showed progressive enrichment in ^{18}O (approximately 0.02‰ per day for the period 2 January 2002 to 30 April 2002) throughout the melt season (see Figure 2). Snowmelt was not sampled during the 2000–2001 melt season; however, the snowpack was approximately 20% less than the long-term mean. Snowpack persistence at PRIMET rarely exceeded 2 weeks during our study period.

[29] The stream $\delta^{18}O$ composition generally reflected the temporal pattern of the precipitation $\delta^{18}O$ composition; however, the signals were significantly damped (Figures 2). The $\delta^{18}O$ standard deviation for stream water varied from 0.11 to 0.34‰, while precipitation standard deviations were 2.98 and 2.80‰ for PRIMET and Hi-15, respectively. The streams each responded to the early portion of the rainy season and showed an enriched isotopic composition reflective of recent rainfall. Winter periods tended to have a more stable isotopic composition approximately equal to the mean value. However, several sites showed significant variability in winter isotopic signals, which might be related to complex snowmelt processes that were not specifically observed in this study. Mean isotopic composition for each stream is significantly elevation-dependent. The elevation effect between the mean catchment elevations and mean isotopic composition was 0.11‰ (r^2 = 0.81; p value = 0.006).

4.2. Residence Time Modeling

[30] Most of the residence time distributions (RTDs) provided satisfactory model simulations to the observed isotopic data (i.e., *E* ranged from 0.2 to 0.6) for all distributions (Table 3). However, only the exponential distribution performed consistently well for all basins (Figure 4). Distributions that contained a mode or did not begin with maximum weighting at the earliest times (e.g., exponential-piston flow distribution and most parameterizations of the dispersion distribution) fit the data poorly (not shown), suggesting that early time rapid response is characteristic of these catchments. Other acceptable distributions for one or several basins included the gamma distribution, two parallel exponential distributions, and power law distribution (see Table 3). The shape parameter, α, optimized for the gamma distribution was approximately 1 for all simulations given the large parameter estimate confidence limits. The gamma distribution with $\alpha = 1$ is equivalent to an exponential distribution (see Table 2). The distribution composed of two parallel exponentials provided model simulations with the highest *E*; however, parameters were not identifiable for any of the catchments. The power law distribution did not perform well overall (lowest *E*) (Table 3). It provided simulations with short-term rapid fluctuations and a long-term flat signal that did not represent the nature of the observed isotopic pattern.

[31] The simulations shown in Figure 4 are the best performing exponential models overall. More importantly,

Table 3. Residence Time Modeling Results[a]

Site	E_R ($\pm 2\sigma_p$),[b] m	Exponential			Gamma				Two Parallel Linear Reservoirs					Power Law		
		τ_m ($\pm 2\sigma_p$), y	E	RMSE, ‰	α ($\pm 2\sigma_p$)	β ($\pm 2\sigma_p$), y	E	RMSE, ‰	τ_f ($\pm 2\sigma_p$),[c] y	τ_s ($\pm 2\sigma_p$),[c] y	ϕ[c]	E	RMSE, ‰	k ($\pm 2\sigma_p$)	E	RMSE, ‰
WS02	647 (±36)	2.2 (±0.56)	0.45	0.11	0.78 (±0.21)	5.5 (±7.55)	0.48	0.10	0.3 (±0.29)	16.5	0.08	0.49	0.10	0.38 (±0.05)	0.47	0.11
WS03	594 (±42)	1.3 (±0.31)	0.48	0.17	0.74 (±0.19)	3.4 (±3.60)	0.53	0.16	0.3 (±0.24)	10.8	0.16	0.52	0.16	0.48 (±0.05)	0.45	0.16
WS08	994 (±32)	3.3 (±1.28)	0.40	0.09	0.96 (±0.23)	3.6 (±2.87)	0.41	0.09	0.5	7.0	0.08	0.40	0.09	0.32 (±0.11)	0.37	0.09
WS09	432 (±50)	0.8 (±0.18)	0.46	0.25	0.92 (±0.22)	1.0 (±0.60)	0.46	0.25	0.3 (±0.20)	21.9	0.24	0.60	0.22	0.53 (±0.08)	0.40	0.26
WS10	474 (±47)	1.2 (±0.29)	0.49	0.19	0.76 (±0.18)	2.6 (±2.12)	0.51	0.19	0.3 (±0.30)	18.7	0.20	0.53	0.19	0.49 (±0.07)	0.43	0.21
MACK	1010 (±28)	2.0 (±0.49)	0.54	0.12	0.97 (±0.17)	2.2 (±1.15)	0.54	0.12	0.3	2.3 (±1.84)	0.04	0.54	0.12	0.37 (±0.08)	0.42	0.14
LOOK	916 (±48)	2.0 (±1.00)	0.32	0.11	1.23 (±0.39)	1.1 (±0.98)	0.36	0.11	0.4	2.0 (±4.91)	0.00	0.32	0.11	0.30 (±0.18)	0.19	0.12

[a]The best fit parameter value, its associated 95% confidence limits (i.e., $2\sigma_p$), measure of efficiency (E), and root mean square error (RMSE) are listed for each model.
[b]Estimated recharge elevation (E_R). Values are only reported for the exponential model since estimates for all other models were similar. Note that E_R estimates for WS08, WS09, and WS10 were not significantly different than their minimum catchment elevation (Table 1); thus the $\delta^{18}O$ in precipitation did not have an elevation effect.
[c]If estimates of the confidence limits are not shown, they were >5 times the parameter estimate; thus the given parameter estimate was ill determined.

they are among the simplest since only one distribution parameter was optimized (i.e., τ_m). The model simulations captured the seasonality of the isotopic data very well, especially the early winter rainfall signal. These periods had the greatest influence on the model calibration as indicated by the temporal nature of τ_m sensitivity and given that is when the largest isotopic deflection occurs. The mean residence times ranged from 0.8 to 3.3 years with 95% confidence limits (i.e., $2\sigma_p$) of 0.18 to 1.28 years (Table 3). The relative age differences among these catchments can be shown by the apparent damping of the input isotopic signal in the observed stream water isotopic signal [cf. *Maloszewski et al.*, 1983; *Herrmann et al.*, 1999]. The relationship between τ_m and the ratio of the standard deviation of stream water isotopic composition to the standard deviation of precipitation isotopic composition, an indication of signal damping, supported the relative age estimates between the catchments (Figure 5). The Nash-Sutcliffe objective measure ranged from 0.32 to 0.54 for the exponential model simulations.

[32] The effective recharge elevations for each catchment were optimized to obtain mass balance between the stream isotopic composition and the input composition given by equation (1). Only WS02, WS03, MACK, and LOOK basins had effective recharge elevations that were higher than the reference precipitation station elevation. Thus only these catchments had significant input isotopic elevation

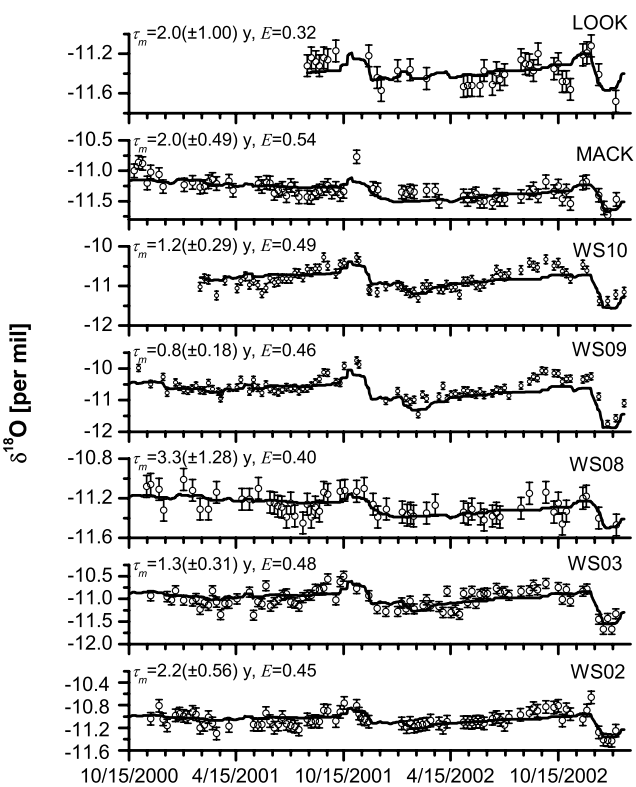

Figure 4. Measured and simulated $\delta^{18}O$ for each catchment using exponential residence time distributions. The estimated mean residence times (τ_m) are shown with 95% confidence limits ($2\sigma_p$) in parentheses, and Nash-Sutcliffe efficiency measures (E) [*Nash and Sutcliffe*, 1970] are shown for model simulation comparisons. Error bars indicate the analytical reproducibility for $\delta^{18}O$ measurements.

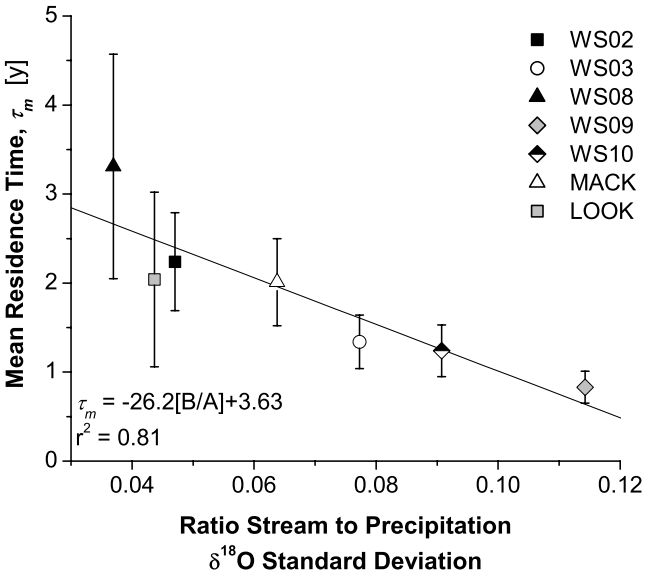

Figure 5. The relationship between mean residence time (τ_m) and ratio of the standard deviations of δ^{18}O measurements of stream water (B) to precipitation (A). Error bars indicate the 95% confidence limits ($2\sigma_p$) of the τ_m parameter estimates.

effects. The remaining catchments (WS08, WS09, and WS10) had effective recharge elevations equal to the elevations of the precipitation collection stations. Effective recharge elevations for WS02, WS03, MACK, and LOOK were between 20 and 40% of the catchment elevation range (647 m, 594 m, 1010 m, and 916 m for WS02, WS03, MACK, and LOOK, respectively). No differences were observed in calibrated effective recharge elevations when other residence time models were used. The effective recharge elevation parameter only changes the input composition to reflect the observed isotopic elevation effects (Figure 2).

[33] The RTDs in Figure 6 illustrate the diverse transport behavior within the overall LOOK drainage. These distributions indicate the relative memory of the catchments to past inputs and thus reflect how long these catchment store and release water or conservative contaminants. The distributions for WS09 and WS10 are more responsive than the other basins, which release between 35% and 42% of the total stored water annually, compared to 70% and 56% for WS09 and WS10, respectively. Not surprisingly, catchments with similar geology/geomorphology had similar RTDs (Table 1).

[34] Since several of the distributions have rather prolonged residence times, the length of the input function must be considered to assess uncertainty. The amount of tracer mass that would pass through these catchments over the timeframe given by the measured portion of the input function (1131 days) is one way to assess the uncertainty of the distribution (shown in Figure 6 where the distribution curves become dashed lines). Therefore, if 100% of the tracer mass exists within the timeframe of the input measurement, then one would have more confidence in the selection of that RTD. The recovered mass at 1131 days was 75, 81, 61, 98, 92, 79, and 78% for WS02, WS03, WS08, WS09, WS10, MACK, and LOOK, respectively. We argue that in addition to parameter estimation error (σ_p), these recovery rates indicate uncertainty caused from the dependence on the extended input data (see section 3.2). For example, 39% of the tracer mass in WS08 originated prior to our observations. Cumulative residence time distributions shown in the inset of Figure 6 further illustrate this point.

4.3. Residence Time and Topographic Analysis

[35] Catchment area showed no apparent relationship to the estimated mean residence times (τ_m) ($r^2 < 0.01$) (Figure 7a). The two largest basin scales, MACK (5.81 km^2) and LOOK (62.42 km^2), had younger τ_m than WS02 (0.601 km^2) and WS08 (0.214 km^2), while catchments with the youngest τ_m were the smallest basins (WS09 and WS10, 0.085 and 0.102 km^2, respectively). Other topographic indices were regressed against the mean residence time, including the accumulation of subcatchment areas (e.g., median subcatchment area, $r^2 < 0.01$), the hypsometric integral ($r^2 = 0.36$, $p = 0.213$), and the mean topographic index ($r^2 = 0.85$, $p < 0.01$). Mean values of the topographic index did not vary significantly between catchments (6.1 to 7.2). Topographic characteristics that described surface flow path attributes were highly correlated to τ_m (see Figure 7; note that WS09 was not included in most of the topographic analyses because the DEM resolution was not sufficient to define the stream channels; however, it was expected to behave similarly to WS10). Even simple measures such as the catchment average slope showed significant correlations with τ_m ($r^2 = 0.78$, $p < 0.01$).

[36] Distributions of flow path lengths and gradients computed from the DEMs provided information regarding the internal arrangement of flow pathways and area accumulation, which are thought to control transport at the gross catchment scale. Figures 7b, 7c, and 7d show the medians of flow path length ($r^2 = 0.72$, $p = 0.03$), flow path gradient ($r^2 = 0.64$, $p = 0.056$), and their ratio (*LG* ratio) (r^2 =

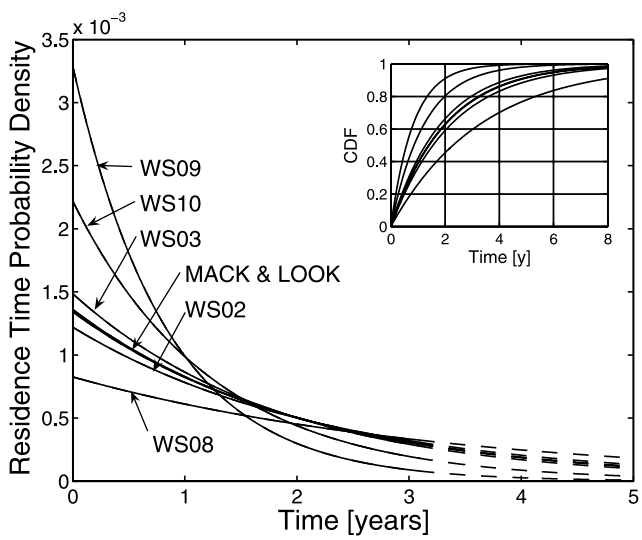

Figure 6. Residence time distributions based on best parameter estimates for each catchment. The solid line designates the length of the study period, and the inset shows the cumulative residence time distributions (CDF) that can be interpreted as mass recovery from an instantaneous, uniform tracer addition.

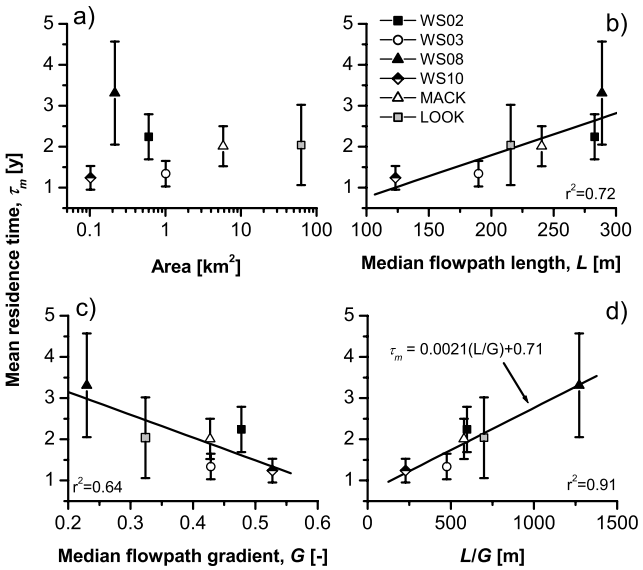

Figure 7. The relationships between mean residence time estimated by modeling $\delta^{18}O$ variations in stream water (equation (4)) and (a) catchment area, (b) median flow path length (L), (c) median flow path gradient (G), and (d) the ratio of median flow path length to median flow path gradient (L/G). Median flow path values were determined from all potential flow paths defined by a DEM analysis. Error bars indicate the 95% confidence limits ($2\sigma_p$) of the τ_m parameter estimates.

0.91, $p < 0.01$) compared to τ_m. The correlation between τ_m and the LG ratio remains high even if WS08 were removed ($r^2 = 0.71$, $p = 0.073$) considering that its τ_m estimate is the most uncertain (i.e., $2\sigma_p = 1.28$ y and only 61% of the tracer mass can be accounted for by the model within the time period of measurements).

5. Discussion

5.1. Residence Time Modeling

[37] The mean and distribution of residence times estimated in this study using stable isotope tracers are not unlike results (1–5 years) found for other small basin (<100 km^2) studies [*Maloszewski et al.*, 1983; *Lindström and Rodhe*, 1986; *Maloszewski et al.*, 1992; *Rodhe et al.*, 1996; *Vitvar and Balderer*, 1997; *Burns et al.*, 1998; *Herrmann et al.*, 1999; *McGuire et al.*, 2002; *Uhlenbrook et al.*, 2002]. However, these studies evaluated residence time for only 1 to 3 catchment scales, as opposed to our investigation that included 7 catchment scales with mean residence time estimates ranging from 0.8 to 3.3 years for basins between 0.085 and 62.42 km^2 in a diverse geomorphic setting. Residence time does not depend on catchment scale. The largest catchment, LOOK, has a residence time that was intermediate to the other basins indicating that its dominant flow sources represent some average contribution of sources that are contained within the other basins. In other words, the overall basin residence time represents an integration of the various subbasin residence times.

[38] The exponential distribution that we used in our residence time modeling represents the simplest possible distribution given that there is only one parameter to estimate for the distribution. Other distributions, while more flexible due to a larger number of parameters, often produced better model simulations (i.e., larger E), but we could not justify using more complex distributions since all or some of the parameters were not identifiable (Table 3). In addition, gamma distributions parameterized to fit these observations were essentially exponential, indicating the exponential distribution of residence times is a good, reasonable approximation given the input-output isotopic data available. The estimated shape parameter (α) for several of the catchments (WS02, WS03, and WS10) was less than 1 suggesting these approach the fractal scaling observed by *Kirchner et al.* [2000]. However, the confidence limits (Table 3) indicate that α was not well identified.

[39] The high variability contained in the stream isotopic data for several of our sites (e.g., WS02, WS08, and LOOK) suggests that more complex processes occur in these basins that cannot be represented in simple lumped parameter models. Nevertheless, these models capture the dominant isotopic pattern over a large range of spatial scales where there is extreme variability in runoff generation and snowmelt processes. *Haitjema* [1995] suggests that the exponential distribution as obtained by assuming steady state Dupuit-Forchheimer flow is independent of catchment size, shape, stream network, and hydraulic conductivity distribution, as long as the saturated zone remains relatively constant. Our analyses seem to support the exponential distribution as a first-order approximation to the true RTD. However, given the extremely damped output $\delta^{18}O$ signal of all sites, rigorous discrimination between models was not possible. Differences in the observed degree of isotopic damping between sites strongly suggest that the relative residence time differences between basins were approximately correct (Figure 5).

[40] Similar model fits have been obtained by other investigators using lumped parameter isotope models [*Maloszewski et al.*, 1992; *Vitvar and Balderer*, 1997; *Uhlenbrook et al.*, 2002; *McGuire et al.*, 2002]. While one can argue that more complex models are warranted for catchment systems, uncertainty in the input composition and parameter estimation of more complex RTDs suggests that models with the fewest degrees of freedom are more practicable [*Maloszewski and Zuber*, 1993, 1998].

5.2. Topographic Relationship

[41] Results from some studies [*Fritz*, 1981; *Burgman et al.*, 1987; *DeWalle et al.*, 1997; *McDonnell et al.*, 1999; *Soulsby et al.*, 2000] have implied that there is a positive correlation between basin area and residence time; however, as shown in this study and other recent studies [*McGuire et al.*, 2002; *McGlynn et al.*, 2003; *Rodgers et al.*, 2005], basin area does not seem to be related to residence time. The strong correlation between mean residence time and simple terrain indices found here suggests that the internal topographic arrangement, as opposed to basin area, may control catchment-scale transport. These results are in contrast to other studies such as that by *Wolock et al.* [1997], who suggested that the spatial pattern of low-flow stream chemistry across basin scale was systematically related to an increase in subsurface contact time (a residence time surrogate) and basin scale. We do not find a consistent relationship between basin scale and residence time in our study.

[42] In areas with significant relief, the flow path distribution at the catchment scale is expected to follow the general topographic form of the basin. The catchment-scale flow path distribution is largely a function of catchment geometry [*Kirchner et al.*, 2001; *Lindgren et al.*, 2004], the spatially variability of contributing areas [*McDonnell et al.*, 1991], and expression of groundwater seepage [*Asano et al.*, 2002]. At the hillslope scale, residence time should increase with accumulated area or flow path length as was observed by *Stewart and McDonnell* [1991] and *Rodhe et al.* [1996]. *Asano et al.* [2002] tested this hypothesis and found that residence time increased only with accumulated area for perennial shallow groundwater defined by bedrock seeps and that transient shallow groundwater in the soil profile appeared to age in a vertical direction (i.e., dependent on soil depth). These studies suggest that even at the hillslope scale, the flow path distribution is quite complex. However, as one moves to the catchment scale, a clear pattern emerges, where residence times increase with flow path length (i.e., catchment geometry) and decrease with flow path gradient (Figure 7). *Buttle et al.* [2001] and *Rodhe et al.* [1996] both found weak correlations between groundwater residence times in various catchment positions and the $\ln(a/\tan\beta)$ index, suggesting similar behavior. Interestingly, the correlation of residence time with L/G is significantly better than the correlation of residence time with flow path length (L) or flow path gradient (G) individually. This suggests that both factors are important controls on residence time.

[43] The relationship between the accumulation of contributing areas and residence time was explored by *McGlynn et al.* [2003]. They found that the mean residence time estimated from tritium data was positively correlated to the median area of all subcatchments that drain to the stream channels (an indication of the portion of area that accumulates as hillslope), but not the true catchment area. Thus catchment area did not accumulate similarly across scales or between catchments of similar size. *McGlynn et al.* [2003] suggested that the distribution of subcatchment areas might be more useful than total catchment area for evaluating watershed function. While, our analysis did not show a significant relationship with median subcatchment area, the LG ratio also suggests that the hillslope and channel network structure are more important controls on transport than total catchment area. The flow path length and gradient distribution reflects the hydraulic driving force of catchment-scale transport (i.e., Darcy's law). Considering the empirical nature of these results and that mean and median are simple characteristics of the distributions, it is clear that some description of topography provides a first-order control on flow processes and transport. The nature of the LG ratio and τ_m relationship is not expected to be similar at other sites. Rather, the slope of the line is expected to change reflecting the relative role of topography and that perhaps other descriptions (e.g., subcatchment area accumulation) are more useful at other sites and regions that show little change in hillslope lengths and gradient. For example, in a recent study by *Rodgers et al.* [2005], τ_m appears to be related to a combination of topography and soil type.

[44] Our observation of strong topographic control on residence time suggests that the HJA flow system is relatively shallow and dominated by topography. Notwithstanding, the residence time results suggest that average storage significantly exceeds approximated average soil depths (τ_m = volume of mobile water (i.e., storage) divided by mean discharge). For example, based on the estimated τ_m for WS10 (1.2 years) and the average annual runoff (1480 mm/y), one would expect approximately 1776 mm of storage. Since soil depths on average for WS10 are between 1 and 3 m and effective porosity ≈ 0.2 [*Ranken*, 1974], then the storage would exceed the capacity of the soil, suggesting that bedrock storage is significant, but still topographically controlled. Similar interpretation can be made for the other HJA catchments, indicating that while topography controls flow, storage in bedrock is significant.

[45] The lack of relationship between basin area and τ_m may indicate differences in the geology and geologic history of the landscape. Average basin slope explains 78% of the variance in τ_m, indicating that it was one of the most important topographic factors in our study. The average slope is also highly correlated to the logarithm of basin area ($r^2 = 0.94$, $p < 0.01$). If WS08 is removed as an outlier, this suggests indirectly, that τ_m is related to basin area provided that geology is generally consistent across basins. In the HJA, lower-elevation basins (WS02, WS03, WS09, WS10) are mostly underlain by the highly weathered Oligocene-lower Miocene volcaniclastic rocks. The topography in these areas is characterized by steeply dissected short hillslopes. Many of the upper elevation small basins in the HJA have been glaciated and/or contain earth flows and thus have gentle topography and longer hillslopes. While our data set is limited to only one catchment in this geologic type (i.e., WS08), these basins do not conform to the log linear relationship between basin slope and area. Therefore correlation between basin area and τ_m may be obscured by geologic differences among basins. Other topographic measures presented herein (e.g., LG ratio) may reflect these geologic features more directly.

5.3. Beyond Small Catchments

[46] Empirical results from this study suggest that the internal form and structure of the basin defines a fundamental control on the catchment-scale residence time. Indeed more multiscale studies focused on residence time and other measures that integrate processes at the catchment scale are necessary to verify relationships such as those presented in this study. However, relationships between topographic measures that can be easily computed from DEMs and residence time may provide a way to regionalize process descriptions of catchments to scales of interest for management, modeling, and biogeochemical studies. Information gathered from intense tracer studies at a limited number of diverse end-member catchments, might be extended to characterize larger systems (i.e., upscaling) or facilitate a more complete understanding of mesoscale systems where measurements that differentiate processes are difficult to obtain [*Uhlenbrook et al.*, 2004; *Soulsby et al.*, 2004].

[47] The RTD is a fundamental descriptor of catchment hydrology. Knowledge of residence time has important implications to how one might define models at the mesoscale where data are limited. In this study, the estimated mean residence times indicate that there is a landscape-level

organization (i.e., topography), which can be used to distribute information regarding average storage or flow velocity. This information can then be used in a priori model development and/or multicriteria model calibration [*Melhorn and Leibundgut*, 1999; *Uhlenbrook et al.*, 2000]. Furthermore, the RTD provides an integrative measure and process description of hillslope complexity at the catchment scale that may be used to infer model structures and advance their predictive capability [*Sivapalan*, 2003].

6. Conclusions

[48] Although residence time has been implicated in other studies to scale with catchment area, this study has shown that the internal form and structure of the catchment, as opposed to absolute catchment area, controls catchment-scale transport. Seemingly simple topographic attributes such as the median flow path length and gradient, which can be computed from any digital elevation model, were strongly correlated to residence time distributions at the catchment scale that represent relatively complex hydrological processes. This relationship allows for the regionalization of residence time and insight to process understanding at the mesoscale. Results from this study suggest that tracers might help bridge the gap between small basins and the mesoscale by providing a linkage between topography, scale, and process. Furthermore, approaches such as the one presented here, provide opportunities to investigate patterns and processes across scale and to offer new perspectives into hydrological and hydrochemical processes that may only become apparent at larger scales.

[49] **Acknowledgments.** This work was supported through funding from the National Science Foundation (grant DEB 021-8088 to the Long-Term Ecological Research Program at the H. J. Andrews Experimental Forest) and Department of Forest Engineering at Oregon State University. We thank C. Creel, G. Downing, and J. Moreau for assistance in the field; D. Henshaw for access to meteorological and streamflow data from the FSDB; and R. Haggerty for suggestions on parameter confidence limits. This manuscript benefited from two anonymous reviews and from helpful comments on an earlier draft by S. Uhlenbrook, J. Jones, and R. Haggerty.

References

Amin, I. E., and M. E. Campana (1996), A general lumped parameter model for the interpretation of tracer data and transit time calculation in hydrologic systems, *J. Hydrol.*, *179*, 1–21.

Anderson, S. P., W. E. Dietrich, D. R. Montgomery, R. Torres, M. E. Conrad, and K. Loague (1997), Subsurface flow paths in a steep, unchanneled catchment, *Water Resour. Res.*, *33*, 2637–2653.

Asano, Y., T. Uchida, and N. Ohte (2002), Residence times and flow paths of water in steep unchannelled catchments, Tanakami, Japan, *J. Hydrol.*, *261*, 173–192.

Bard, Y. (1974), *Nonlinear Parameter Estimation*, 341 pp., Elsevier, New York.

Berris, S. N., and R. D. Harr (1987), Comparative snow accumulation and melt during rainfall in forested and clear-cut plots in the western Cascades of Oregon, *Water Resour. Res.*, *23*, 135–142.

Bethke, C. M., and T. M. Johnson (2002), Technical commentary: Ground water age, *Ground Water*, *40*(4), 337–339.

Beven, K. J., and M. J. Kirkby (1979), A physically based, variable contributing area model of basin hydrology, *Hydrol. Sci. Bull.*, *24*(1), 43–69.

Bonell, M. (1998), Selected challenges in runoff generation research in forests from the hillslope to headwater drainage basin scale, *J. Am. Water Resour. Assoc.*, *34*(4), 765–786.

Burgman, J. O., B. Calles, and F. Westman (1987), Conclusions from a ten year study of oxygen-18 in precipitation and runoff in Sweden, in *Isotope Techniques in Water Resources Development, an International Symposium*, pp. 579–590, Int. At. Energy Agency, Vienna.

Burns, D. A., and J. J. McDonnell (1998), Effects of a beaver pond on runoff processes: Comparison of two headwater catchments, *J. Hydrol.*, *205*, 248–264.

Burns, D. A., P. S. Murdoch, G. B. Lawrence, and R. L. Michel (1998), Effect of groundwater springs on NO_3^- concentrations during summer in Catskill Mountain streams, *Water Resour. Res.*, *34*, 1987–1996.

Burns, D. A., et al. (2003), The geochemical evolution of riparian ground water in a forested piedmont catchment, *Ground Water*, *41*(7), 913–925.

Buttle, J. M. (1994), Isotope hydrograph separations and rapid delivery of pre-event water from drainage basins, *Prog. Phys. Geogr.*, *18*(1), 16–41.

Buttle, J. M., P. W. Hazlett, C. D. Murray, I. F. Creed, D. S. Jeffries, and R. Semkin (2001), Prediction of groundwater characteristics in forested and harvested basins during spring snowmelt using a topographic index, *Hydrol. Processes*, *15*, 3389–3407.

Chorley, R. J., S. A. Schumm, and D. E. Sugden (1985), *Geomorphology*, 605 pp., Methuen, London.

Clark, I. D., and P. Fritz (1997), *Environmental Isotopes in Hydrogeology*, 328 pp., A. F. Lewis, Boca Raton, Fla.

Coleman, T. F., and Y. Li (1994), On the convergence of reflective Newton methods for large-scale nonlinear minimization subject to bounds, *Math. Program.*, *67*(2), 189–224.

Dansgaard, W. (1964), Stable isotopes in precipitation, *Tellus*, *16*, 436–438.

DeWalle, D. R., P. J. Edwards, B. R. Swistock, R. Aravena, and R. J. Drimmie (1997), Seasonal isotope hydrology of three Appalachian forest catchments, *Hydrol. Processes*, *11*, 1895–1906.

Dinçer, T., and G. H. Davis (1984), Application of environmental isotope tracers to modeling in hydrology, *J. Hydrol.*, *68*, 95–113.

Dinçer, T., B. R. Payne, T. Florkowski, J. Martinec, and E. G. E. I. Tongiorgi (1970), Snowmelt runoff from measurements of tritium and oxygen-18, *Water Resour. Res.*, *6*, 110–124.

Donaldson, J. R., and R. B. Schnabel (1987), Computational experience with confidence regions and confidence intervals for nonlinear least squares, *Technometrics*, *29*(1), 67–82.

Dooge, J. C. I. (1973), *Linear Theory of Hydrologic Systems*, 327 pp., U.S. Gov. Print. Off., Washington, D. C.

Dyrness, C. T. (1969), Hydrologic properties of soils on three small watersheds in the western Cascades of Oregon, *Res. Note PNW-111*, Pac. Northwest For. and Range Exp. Stn., For. Serv., U.S. Dep. of Agric., Portland, Oreg.

Epstein, S., and T. Mayeda (1953), Variation of ^{18}O content of water from natural sources, *Geochim. Cosmochim. Acta*, *4*, 213–224.

Etcheverry, D., and P. Perrochet (1999), Reservoir theory, groundwater transit time distributions, and lumped parameter models, paper presented at International Symposium on Isotope Techniques in Water Resources Development and Management, Int. At. Energy Agency, Vienna, 10–14 May.

Fritz, P. (1981), River waters, in *Stable Isotope Hydrology: Deuterium and Oxygen-18 in the Water Cycle*, *Tech. Rep. Ser. 210*, edited by J. Gat and R. Gonfiantini, pp. 177–201, Int. At. Energy Agency, Vienna.

Gibson, J. J., et al. (2002), Isotope studies in large river basins: A new global research focus, *Eos Trans. AGU*, *83*(52), 616.

Grabczak, J., P. Maloszewski, K. Rozanski, and A. Zuber (1984), Estimation of the tritium input function with the aid of stable isotopes, *Catena*, *11*, 105–114.

Haggerty, R., S. W. Fleming, L. C. Meigs, and S. A. McKenna (2001), Tracer tests in a fractured dolomite: 2. Analysis of mass transfer in single-well injection-withdrawal tests, *Water Resour. Res.*, *37*, 1129–1142.

Haitjema, H. M. (1995), On the residence time distribution in idealized groundwatersheds, *J. Hydrol.*, *172*(1–4), 127–146.

Harr, R. D. (1977), Water flux in soil and subsoil on a steep forested slope, *J. Hydrol.*, *33*, 37–58.

Harr, R. D. (1986), Effects of clearcutting on rain-on-snow runoff in western Oregon: A new look at old studies, *Water Resour. Res.*, *22*, 1095–1100.

Harr, R. D., and F. M. McCorison (1979), Initial effects of clearcut logging on size and timing of peak flows in a small watershed in western Oregon, *Water Resour. Res.*, *15*, 90–94.

Herrmann, A., S. Bahls, W. Stichler, F. Gallart, and J. Latron (1999), Isotope hydrological study of mean transit times and related hydrogeological conditions in Pyrenean experimental basins (Vallcebre, Catalonia), in *Integrated Methods in Catchment Hydrology—Tracer, Remote Sensing, and New Hydrometric Techniques (Proceedings of IUGG 99 Symposium HS4)*, edited by C. Leibundgut, J. McDonnell, and G. Schultz, *IAHS Publ.*, *258*, 101–110.

Hewlett, J. D., and A. R. Hibbert (1967), Factors affecting the response of small watersheds to precipitation in humid areas, in *Forest Hydrology*, edited by W. E. Sopper and H. W. Lull, pp. 275–291, Elsevier, New York.

Hooper, R. P. (2001), Applying the scientific method to small catchment studies: A review of the Panola Mountain experience, *Hydrol. Processes*, *15*, 2039–2050.

Hooper, R. P. (2004), Designing observatories for the hydrologic sciences, *Eos Trans. AGU*, *85*(17), Jt. Assem. Suppl., Abstract H24B-04.

Hornberger, G. M., T. M. Scanlon, and J. P. Raffensperger (2001), Modelling transport of dissolved silica in a forested headwater catchment: The effect of hydrological and chemical time scales on hysteresis in the concentration-discharge relationship, *Hydrol. Processes*, *15*, 2029–2038.

Ingraham, N. L. (1998), Isotopic variation in precipitation, in *Isotope Tracers in Catchment Hydrology*, edited by C. Kendall and J. J. McDonnell, pp. 87–118, Elsevier, New York.

Jones, J. A. (2000), Hydrologic processes and peak discharge response to forest removal, regrowth, and roads in 10 small experimental basins, western Cascades, Oregon, *Water Resour. Res.*, *36*, 2621–2642.

Jones, J. A., and G. E. Grant (1996), Peak flow responses to clear-cutting and roads in small and large basins, western Cascades, Oregon, *Water Resour. Res.*, *32*, 959–974.

Kendall, C., and J. J. McDonnell (1998), *Isotope Tracers in Catchment Hydrology*, 839 pp., Elsevier, New York.

Kirchner, J. W. (2003), A double paradox in catchment hydrology and geochemistry, *Hydrol. Processes*, *17*, 871–874.

Kirchner, J. W., X. Feng, and C. Neal (2000), Fractal stream chemistry and its implications for contaminant transport in catchments, *Nature*, *403*(6769), 524–527.

Kirchner, J. W., X. Feng, and C. Neal (2001), Catchment-scale advection and dispersion as a mechanism for fractal scaling in stream tracer concentrations, *J. Hydrol.*, *254*, 82–101.

Knopman, D. S., and C. I. Voss (1987), Behavior of sensitivities in the one-dimensional advection-dispersion equation: Implications for parameter estimation and sampling design, *Water Resour. Res.*, *23*(2), 253–272.

Kreft, A., and A. Zuber (1978), On the physical meaning of the dispersion equation and its solutions for different initial and boundary conditions, *Chem. Eng. Sci.*, *33*, 1471–1480.

Legard, H. A., and L. C. Meyer (1973), *Soil Resource Inventory, Atlas of Maps and Interpretive Tables*, *Willamette National Forest*, Pac. Northwest Region, U.S. For. Serv., Portland, Oreg.

Lindgren, G. A., G. Destouni, and A. V. Miller (2004), Solute transport through the integrated groundwater-stream system of a catchment, *Water Resour. Res.*, *40*, W03511, doi:10.1029/2003WR002765.

Lindström, G., and A. Rodhe (1986), Modelling water exchange and transit times in till basins using oxygen-18, *Nord. Hydrol.*, *17*(4–5), 325–334.

Maloszewski, P., and A. Zuber (1982), Determining the turnover time of groundwater systems with the aid of environmental tracers. 1. Models and their applicability, *J. Hydrol.*, *57*, 207–231.

Maloszewski, P., and A. Zuber (1993), Principles and practice of calibration and validation of mathematical models for the interpretation of environmental tracer data, *Adv. Water Resour.*, *16*, 173–190.

Maloszewski, P., and A. Zuber (1998), A general lumped parameter model for the interpretation of tracer data and transit time calculation in hydrologic systems (*Journal of Hydrology 179* (1996) 1–21), comments, *J. Hydrol.*, *204*, 297–300.

Maloszewski, P., W. Rauert, W. Stichler, and A. Herrmann (1983), Application of flow models in an alpine catchment area using tritium and deuterium data, *J. Hydrol.*, *66*, 319–330.

Maloszewski, P., W. Rauert, P. Trimborn, A. Herrmann, and R. Rau (1992), Isotope hydrological study of mean transit times in an alpine basin (Wimbachtal, Germany), *J. Hydrol.*, *140*, 343–360.

McDonnell, J. J., M. K. Stewart, and I. F. Owens (1991), Effect of catchment-scale subsurface mixing on stream isotopic response, *Water Resour. Res.*, *27*, 3065–3073.

McDonnell, J., L. K. Rowe, and M. K. Stewart (1999), A combined tracer-hydrometric approach to assess the effect of catchment scale on water flow path, source and age, in *Integrated Methods in Catchment Hydrology—Tracer, Remote Sensing, and New Hydrometric Techniques (Proceedings of IUGG 99 Symposium HS4)*, edited by C. Leibundgut, J. McDonnell, and G. Schultz, *IAHS Publ.*, *258*, 265–273.

McGlynn, B. L., and J. Seibert (2003), Distributed assessment of contributing area and riparian buffering along stream networks, *Water Resour. Res.*, *39*(4), 1082, doi:10.1029/2002WR001521.

McGlynn, B. L., J. J. McDonnell, and D. D. Brammer (2002), A review of the evolving perceptual model of hillslope flowpaths at the Maimai catchments, New Zealand, *J. Hydrol.*, *257*, 1–26.

McGlynn, B., J. McDonnell, M. Stewart, and J. Seibert (2003), On the relationships between catchment scale and streamwater mean residence time, *Hydrol. Processes*, *17*, 175–181.

McGuire, K. J., D. R. DeWalle, and W. J. Gburek (2002), Evaluation of mean residence time in subsurface waters using oxygen-18 fluctuations during drought conditions in the mid-Appalachians, *J. Hydrol.*, *261*, 132–149.

Melhorn, J., and C. Leibundgut (1999), The use of tracer hydrological time parameters to calibrate baseflow in rainfall-runoff modelling, in *Integrated Methods in Catchment Hydrology—Tracer, Remote Sensing, and New Hydrometric Techniques (Proceedings of IUGG 99 Symposium HS4)*, edited by C. Leibundgut, J. McDonnell, and G. Schultz, *IAHS Publ.*, *258*, 119–125.

Montgomery, D. R., and W. E. Dietrich (1988), Where do channels begin?, *Nature*, *336*, 232–234.

Nash, J. E., and J. V. Sutcliffe (1970), River flow forecasting through conceptual models, I, A discussion of principles, *J. Hydrol.*, *10*, 282–290.

Pearce, A. J., M. K. Stewart, and M. G. Sklash (1986), Storm runoff generation in humid headwater catchments: 1. Where does the water come from?, *Water Resour. Res.*, *22*, 1263–1272.

Ranken, D. W. (1974), Hydrologic properties of soil and subsoil on a steep, forested slope, M.S. thesis, Oreg. State Univ., Corvallis.

Ratkowsky, D. A. (1990), *Handbook of Nonlinear Regression Models*, 241 pp., CRC Press, Boca Raton, Fla.

Richey, D. G., J. J. McDonnell, M. W. Erbe, and T. M. Hurd (1998), Hydrochemical separation based on chemical and isotopic concentrations: A critical appraisal of published studies from New Zealand, North America, and Europe, *J. Hydrol. N. Z.*, *37*(2), 95–111.

Richter, J., P. Szymczak, T. Abraham, and H. Jordan (1993), Use of combinations of lumped parameter models to interpret groundwater isotopic data, *J. Contam. Hydrol.*, *14*(1), 1–13.

Rodgers, P., C. Soulsby, and S. Waldron (2005), Stable isotope tracers as diagnostic tools in upscaling flow path understanding and residence time estimates in a mountainous mesoscale catchment, *Hydrol. Processes*, in press.

Rodhe, A., L. Nyberg, and K. Bishop (1996), Transit times for water in a small till catchment from a step shift in the oxygen 18 content of the water input, *Water Resour. Res.*, *32*(12), 3497–3511.

Rothacher, J. (1965), Streamflow from small watersheds on the western slope of the Cascade Range of Oregon, *Water Resour. Res.*, *1*, 125–134.

Rothacher, J., C. T. Dyrness, and R. L. Fredriksen (1967), Hydrologic and related characteristics of three small watersheds in the Oregon Cascades, report, Pac. Northwest For. and Range Exp. Stn., For. Serv., U.S. Dep. of Agric., Portland, Oreg.

Schumer, R., D. A. Benson, M. M. Meerschaert, and B. Baeumer (2003), Fractal mobile/immobile solute transport, *Water Resour. Res.*, *39*(10), 1296, doi:10.1029/2003WR002141.

Sherrod, D. R., and J. G. Smith (2000), Geologic map of upper Eocene to Holocene volcanic and related rocks of the Cascade Range, Oregon, *U.S. Geol. Surv. Geol. Invest. Ser. Map, I-2569*.

Sidle, R. C., Y. Tsuboyama, S. Noguchi, I. Hosoda, M. Fujieda, and T. Shimizu (2000), Stormflow generation in steep forested headwaters: A linked hydrogeomorphic paradigm, *Hydrol. Processes*, *14*, 369–385.

Sivapalan, M. (2003), Process complexity at hillslope scale, process simplicity at the watershed scale: Is there a connection?, *Hydrol. Processes*, *17*, 1037–1041.

Sollins, P., C. C. Grier, F. M. McCorison, K. J. Cromack, R. Fogel, and R. L. Fredriksen (1980), The internal element cycles of an old-growth Douglas-fir ecosystem in western Oregon, *Ecol. Monogr.*, *50*, 261–285.

Soulsby, C., R. Malcolm, R. C. Ferrier, R. C. Helliwell, and A. Jenkins (2000), Isotope hydrology of the Allt a'Mharcaidh catchment, Cairngorms, Scotland: Implications for hydrological pathways and residence times, *Hydrol. Processes*, *14*, 747–762.

Soulsby, C., P. J. Rodgers, J. Petry, D. M. Hannah, I. A. Malcolm, and S. M. Dunn (2004), Using tracers to upscale flow path understanding in mesoscale mountainous catchments: Two examples from Scotland, *J. Hydrol.*, *291*, 174–196.

Stewart, M. K., and J. J. McDonnell (1991), Modeling base flow soil water residence times from deuterium concentrations, *Water Resour. Res.*, *27*, 2681–2693.

Strahler, A. N. (1952), Hypsometric (area-altitude) analysis of erosional topography, *Geol. Soc. Am. Bull.*, *63*, 1117–1142.

Swanson, F. J., and M. E. James (1975), Geology and geomorphology of the H.J. Andrews Experimental Forest, western Cascades, Oregon, *Res. Pap. PNW-188*, Pac. Northwest For. and Range Exp. Stn., For. Serv., U.S. Dep. of Agric., Portland, Oreg.

Uhlenbrook, S., C. Leibundgut, and P. Maloszewski (2000), Natural tracer for investigating residence times, runoff components and validation of a rainfall-runoff model, in *TraM'2000: Conference on Tracer and Modelling in Hydrogeology*, *IAHS Publ.*, *262*, 465–472.

Uhlenbrook, S., M. Frey, C. Leibundgut, and P. Maloszewski (2002), Hydrograph separations in a mesoscale mountainous basin at event and seasonal timescales, *Water Resour. Res.*, *38*(6), 1096, doi:10.1029/2001WR000938.

Uhlenbrook, S., S. Roser, and N. Tilch (2004), Hydrological process representation at the mesoscale: The potential of a distributed, conceptual catchment model, *J. Hydrol.*, *291*, 278–296.

Vitvar, T., and W. Balderer (1997), Estimation of mean water residence times and runoff generation by ^{18}O measurements in a pre-Alpine catchment (Rietholzbach, eastern Switzerland), *Appl. Geochem.*, *12*(6), 787–796.

Weiler, M., B. L. McGlynn, K. J. McGuire, and J. J. McDonnell (2003), How does rainfall become runoff? A combined tracer and runoff transfer function approach, *Water Resour. Res.*, *39*(11), 1315, doi:10.1029/2003WR002331.

Welker, J. M. (2000), Isotopic ($\delta^{18}O$) characteristics of weekly precipitation collected across the USA: An initial analysis with application to water source studies, *Hydrol. Processes*, *14*, 1449–1464.

Williams, A. G., J. F. Dowd, and E. W. Meyles (2002), A new interpretation of kinematic stormflow generation, *Hydrol. Processes*, *16*, 2791–2803.

Wolock, D. M., J. Fan, and G. B. Lawrence (1997), Effects of basin size on low-flow stream chemistry and subsurface contact time in the Neversink River watershed, New York, *Hydrol. Processes*, *11*, 1273–1286.

Zuber, A. (1986), On the interpretation of tracer data in variable flow systems, *J. Hydrol.*, *86*, 45–57.

C. Kendall, U.S. Geological Survey, Menlo Park, CA 94025, USA.

J. J. McDonnell, Department of Forest Engineering, Oregon State University, Corvallis, OR 97331, USA.

B. L. McGlynn, Department of Land Resources and Environmental Sciences, Montana State University, Bozeman, MT 59717, USA.

K. J. McGuire, School of Civil and Environmental Engineering, Georgia Institute of Technology, Atlanta, GA 30332-0355, USA. (kevin.mcguire@ce.gatech.edu)

J. Seibert, Department of Physical Geography and Quaternary Geology, Stockholm University, SE-106 91 Stockholm, Sweden.

M. Weiler, Department of Forest Resources Management, University of British Columbia, Vancouver, BC, Canada V6T 1Z4.

J. M. Welker, Environment and Natural Resources Institute, University of Alaska Anchorage, Anchorage, AK 99508, USA.